PHYSICAL REVIEW B VOLUME 32, NUMBER 4 15 AUGUST 1985

Importance of multiple forward scattering in medium- and high-energy electron emission and/or diffraction spectroscopies

S. Y. Tong, H. C. Poon, and D. R. Snider
Laboratory for Surface Studies and Department of Physics, University of Wisconsin—Milwaukee, Milwaukee, Wisconsin 53201

(Received 26 February 1985)

We examine the role of multiple scattering in emission and/or diffraction spectroscopies that involve medium- and high-energy electrons. We use quantum-mechanical and classical methods to demonstrate the importance of multiple forward scattering in these techniques. Single-scattering theory produces errors because it neglects multiple forward scattering from atoms which shadow other atoms.

I. INTRODUCTION

Recent advances in surface techniques have resulted in the development of a number of surface-analytical tools in which the emission and/or scattering of medium- (200—1000 eV) and high- (1000—20 000 eV) energy electrons are involved.[1] These surface spectroscopies can be divided into two classes: (i) those which collect electrons in a forward-direction cone, e.g., angle-resolved x-ray photoemission spectroscopy (XPS),[2–6] Auger-electron spectroscopy (AES),[4–6] and reflection high-energy electron diffraction (RHEED);[1] or (ii) those which collect electrons in large backscattering angles, e.g., angle-resolved energy-dependent photoelectron diffraction (EDPD).[7–10] Considerable effort has been applied in using single-scattering theory to compute intensities and compare them with the measured data.[11–17] In this paper, we question the accuracy of single-scattering theory for evaluating intensities of these medium- and high-energy electron spectroscopies.

II. FORWARD-DIRECTION SURFACE SPECTROSCOPIES

The first techniques examined are forward-direction angle-resolved XPS and AES,[2–6,15–17] in which the emission from a core level of an atom in the surface region is measured as a function of polar angle from the surface normal. The data show intense peaks along directions of nearest-neighbor internuclear axes. It was shown[15] that these peaks are due to focusing of electrons as they pass through the attractive Coulomb potential of an atom. The energy at which forward-direction focusing starts depends on details of the potential, and for copper atoms, the focusing starts at energies $E_k \geq 60$ eV.[15] We show in the following that, because of the focusing effect itself, it is necessary to include multiple forward-scattering to evaluate quantitatively the intensity of this peak. Single-scattering theory produces incorrect results for atoms in deeper layers and its predictions are quantitatively inconsistent with the measured data.

The wave function at $\mathbf{R}$ due to emission from a core level of an atom located at $\mathbf{R}_0$ is given by the multiple-scattering photoemission of Tong *et al.*[18–21] as

$$\begin{aligned}\psi(\mathbf{R}) &= \frac{2m}{\hbar^2} ik_0 \sum_{L} (-i)^{-l} h_l^{(1)}(k_0|\mathbf{R}-\mathbf{R}_0|) Y_L(\mathbf{R}-\mathbf{R}_0) M_L^0 \\ &\quad + \frac{2m}{\hbar^2} ik_0 \sum_{L,L'} (-i)^{-l'} h_{l'}^{(1)}(k_0|\mathbf{R}-\mathbf{R}_0|) Y_{L'}(\mathbf{R}-\mathbf{R}_0) \sum_{i,j=0}^{\infty} (T^{ij}G^{j0})_{L'L} M_L^0 \\ &= \sum_{\mathbf{k}^+} C(\mathbf{k}^+) e^{i\mathbf{k}^+\cdot\mathbf{R}} ,\end{aligned} \tag{1}$$

where k_0 is the magnitude of the photoelectron momentum, $h_l^{(1)}$ is the spherical Hankel function of the first kind, T^{ij} and G^{j0} are multilayer scattering matrices and structural propagators defined in Ref. 20, and the emission atom is located in layer 0. The photon-electron excitation matrix element is defined as

$$\begin{aligned}M_L^0 &= (-i)^l \int d^3r\, e^{i\delta_l^0} R_l^f(|\mathbf{r}-\mathbf{R}_0|) \\ &\quad \times Y_L^*(\mathbf{r}-\mathbf{R}_0) i\hbar \frac{e}{mc} \frac{1}{\epsilon_f-\epsilon_i} \mathbf{A}\cdot\nabla V(\mathbf{r}) \phi_i(\mathbf{r}) .\end{aligned} \tag{2}$$

In the above equation, δ_l^0 is the lth phase shift of the emitting atom at final energy ϵ_f, $R_l^f(r)$ is the normalized radial wave function at energy ϵ_f inside an emission atom, and $\phi_i(\mathbf{r})$ is the initial-state wave function of the electron at energy ϵ_i. Then, from Ref. 20, the differential photoemission cross section $dP/d\Omega$, which is the number of photoelectrons collected in $d\Omega$ per second divided by the incident photon flux, is

$$\frac{dP}{d\Omega} \propto |k_f^{\text{out}}| (k_f^{\text{out}})^2 \frac{1}{\omega_{\text{ph}}} |C(\mathbf{k}_f^+)|^2 , \tag{3}$$

where $\mathbf{k}_f^{\text{out}}$ is the outside electron momentum in the direc-

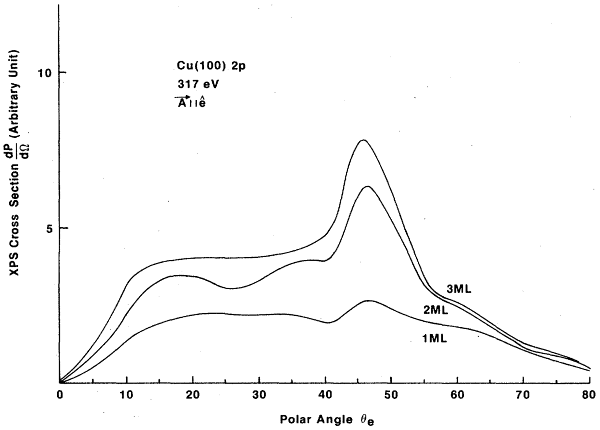

FIG. 1. Angle-resolved XPS cross section, calculated by multiple-scattering theory, for $2p$ Cu(001), at 317 eV, as a function of emission polar angle. The photon **A** vector is along the emission direction and $\theta=0°$ is the direction of the surface normal. The emission plane is (100); ML means monolayer.

tion **R** and ω_{ph} is the photon frequency.

In Fig. 1 we show the XPS cross section $dP/d\Omega$ for Cu(001) at 317 eV, for emission from the $2p$ state, for one, two, and three monolayers (ML). The multiple-scattering formulas (1)—(3) are used. From the figure we see that the internuclear peak at 45°[22] is enhanced by a factor of 2.4 going from 1 to 2 ML, but then further enhancement becomes *much more moderate* going from 2 to 3 ML. The heights of the internuclear peak for 2 and 3 ML, normalized by that of 1 ML, are tabulated in Table I for results using multiple-scattering theory, single-scattering theory (with spherical-wave and plane-wave formulas), and the data of Egelhoff.[4–6] In single-scattering theory, the spherical-wave formula evaluates Hankel functions between emitting and scattering atoms exactly, while the plane-wave formula retains only the first term in the $1/\rho$ expansion of Hankel functions.[15,23] Comparing with the data, spherical-wave single-scattering theory works for 2 ML, plane-wave single-scattering theory fails even there, and only the multiple-scattering result adequately reproduces the emission intensity for the 3-ML case. The single-scattering spherical-wave result overestimates the 3-ML case by 48%, while the plane-wave result overestimates it by 128%. In Table I we also compare results of (spherical-wave) single-scattering theory using 20 partial waves [column (d)] with those of eight partial waves [column (c)]. The comparison shows that at 317 eV, results of eight partial waves have converged to an accuracy of 4%. The multiple-scattering calculations [column (b)] were done with eight partial waves.

Relative contributions to the internuclear peak from individual layers, at a range of energies between 250 to 400 eV, are tabulated in Table II. The tabulated numbers are ratios of the second- and third-monolayer emission contributions to that of the first-monolayer, using multiple-scattering and single-scattering theories. The numbers show that with multiple scattering, the third-layer contribution is rather small, being about 30—50 % of that of the second layer. Single-scattering theory (spherical-wave) on the other hand, overestimates the third-layer contribution at these energies, with values of the third-layer contribution ranging from about equal to bigger than that of the second layer. These numbers illustrate an important physical effect which is correctly described by multiple-scattering theory, but not by single-scattering theory: An electron emitted from a third-layer atom, after being focused into the forward direction by a second-layer atom, is further deflected (and hence *defocused*) to directions other than forward by an atom in the first layer. In multiple-scattering theory, such electrons are *discarded* from the forward-direction peak. In single-scattering theory, however, the *defocusing* effect is neglected because it is a second-order scattering event. As a consequence, single-scattering theory overestimates the forward-direction peak in cases of three or more monolayers, at these energies.

We can illustrate the essence of multiple scattering in the forward direction by the trajectories of classical scattering. Since this is only used for illustration, a simple form of the potential is chosen, i.e., a cutoff Coulomb potential given by[24]

TABLE I. Normalized XPS cross section at $\theta=45°$ for combined emissions from one, two, and three monolayers of Cu(001), at 317 eV, $2p$ emission. The intensities are normalized to unity for the 1-ML case. The experimental numbers are taken from Ref. 6.

Monolayers	(a) Expt.	(b) Multiple scattering	(c)	(d)	(e) Single scattering (plane wave)
			Single scattering (spherical wave)		
1	1	1	1	1	1
2	2.3	2.35	2.46	2.50	3.40
3	2.7	2.97 (8 partial waves)	4.0 (8 partial waves)	4.15 (20 partial waves)	6.16 (20 partial waves)

TABLE II. Normalized XPS cross section for emission from an atom located in the (a) surface layer, (b) second layer, and (c) third layer, respectively. The intensity of emission from an atom in the surface layer is normalized to unity.

Energy (eV)	Multiple scattering (8 partial waves)	Spherical-wave single scattering (8 partial waves)
250	(a) 1.00	1.00
	(b) 1.6	1.37
	(c) 0.66	1.21
300	(a) 1.00	1.00
	(b) 1.52	1.42
	(c) 0.66	1.43
317	(a) 1.00	1.00
	(b) 1.35	1.46
	(c) 0.62	1.54
350	(a) 1.00	1.00
	(b) 1.91	1.50
	(c) 1.01	1.59
400	(a) 1.00	1.00
	(b) 1.22	1.30
	(c) 0.60	1.44

$$V(r)=\begin{cases} Z(1/r-1/a), & r<a \qquad (4a)\\ 0, & r\geq a\,. \qquad (4b)\end{cases}$$

Here a is the radius of the atom. The trajectories of the classical electrons are then straight lines in the region between the potentials and hyperbolas inside the potentials. The equation of a hyperbolic trajectory is

$$r(\theta)=\frac{(\epsilon^2-1)c}{1+\epsilon\cos(\theta-\theta_0)}\,,\quad r<a \tag{5}$$

where for the above potential

$$c=\frac{Za}{2(Ea-Z)}\,. \tag{6}$$

The two parameters ϵ and θ_0 are determined by the position and angle of the straight part of the incident trajectory. That is, in Fig. 2, γ and ω determine ϵ and θ_0 which, in turn, through Eq. (5), fix where and at what angle the electron emerges from the atom. We only consider cases where the incident ray and the centers of all the atoms involved lie in a single plane; thus the entire trajectory will stay in this plane.

Using the classical method, the trajectories of electrons at 317 eV (for $Z=30$) are shown in Fig. 3(a). Reading from right to left, ray A' is focused into the forward direction by atom 1, but is then deflected to a new direction (ray A) by atom 2. Ray B, on the other hand, exits atom 1 at an oblique angle, but is then focused into the forward direction by atom 2. Thus, multiple scattering defocuses the ray chosen in single-scattering theory (ray A'), and instead, introduces a new ray into the forward direction (ray B). Single-scattering theory also contains a third ray: an electron, unscattered by atom 1, enters atom 2 and is forward focused by it. There is no counterpart of this ray in multiple-scattering theory.

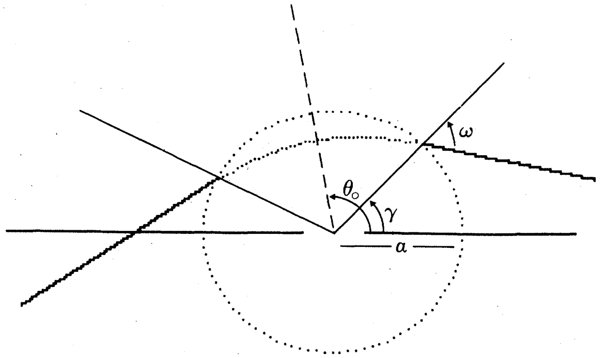

FIG. 2. Classical electron trajectory due to scattering by a cutoff Coulomb potential.

The situation illustrated in Fig. 3(a) corresponds to emission from an atom in the third monolayer. To compare the results of multiple scattering and single scattering, we define a ratio of count rates, τ, as ratio of the number of electrons per second scattered into a circular detector in the forward direction with $\Delta\theta=1°$ to the number of electrons emitted by the source each second directly into the same detector. For scattering by one atom, $\tau_{A'}$ is 5.04, and for two atoms, τ_B drops down to 1.38.[25] Since $\tau_{A'}$ is included in single-scattering theory, it follows that the two-atom classical count rate evaluated by single-scattering theory is much larger than that by multiple-scattering theory (τ_B), a result in agreement with the quantum-mechanical result.

The classical scattering model shows that multiple scattering is still important at 1000 eV (the data by Egelhoff[4-6] for forward-direction AES are taken at 917 eV).

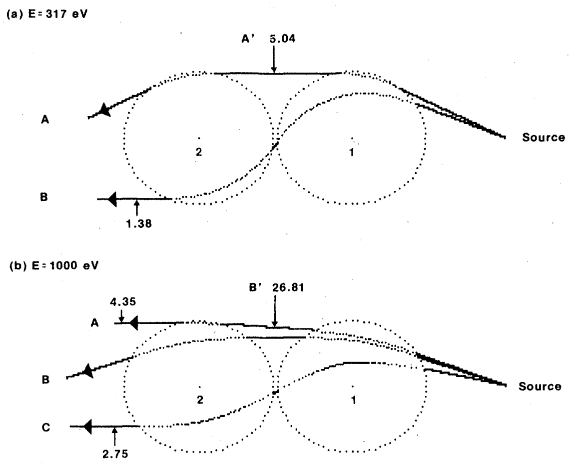

FIG. 3. Classical trajectories for forward focusing of electrons emitted from a point source by two atoms: (a) electron energy = 317 eV and (b) electron energy = 1000 eV. The number on each ray is the classical count rate τ.

Here, as shown in Fig. 3(b), the path picked by single scattering (ray B'), which has $\tau_{B'}=26.81$, is defocused to ray B by scattering at atom 2. Two multiple-scattering paths, rays A and C, focused electrons into the forward direction, with combined $\tau_{A+C}=7.1$. The classical count rate, because it disregards interference between paths (e.g., A and C), can be viewed as the mean over energy of variations in the quantum-mechanical results. Classical theory is also known to break down for Coulomb potentials at very high energies.

A similar situation exists for the surface spectroscopy, RHEED, where high-energy electrons are elastically scattered by rows of surface atoms and are collected at small forward-direction angles. The role of multiple scattering can be illustrated by the classical analog of a parallel beam of electrons scattering from a row of atoms aligned along the beam direction. We show in Figs. 4(a) and 4(b) the scattering of electrons at 1000 and 20 000 eV, respectively, by one and two atoms, at a scattering angle $\theta_s=10°$. At the lower energy (i.e., $E_k=1000$ eV), the combined scattering cross section $d\sigma/d\Omega$ (the number of electrons scattered into $d\Omega$ per second per unit incident electron flux) of two atoms is much less than the cross section of one atom (1.98 Å^2 versus 7.0 Å^2). At the higher energy (i.e., $E_k=20\,000$ eV), the multiple-scattering path C [Fig. 4(b)] becomes dominant. The combined two-atom cross section is 4.14 times larger than that of the single atom (2.11 versus 0.51). At either the low or high energy, the multiple-scattering result is very different from the single-scattering prediction: The latter requires that the combined two-atom cross section be twice that of one atom. Therefore, to evaluate RHEED intensities due to scattering of electrons by a row of atoms in the direction of, or at small angles from, the incident beam, one must use a quantum-mechanical multiple-forward-direction-scattering theory.[26,27] Masud and Pendry have developed a chain method to take care of multiple scattering in RHEED along chains of atoms in directions close to the incident beam.[28]

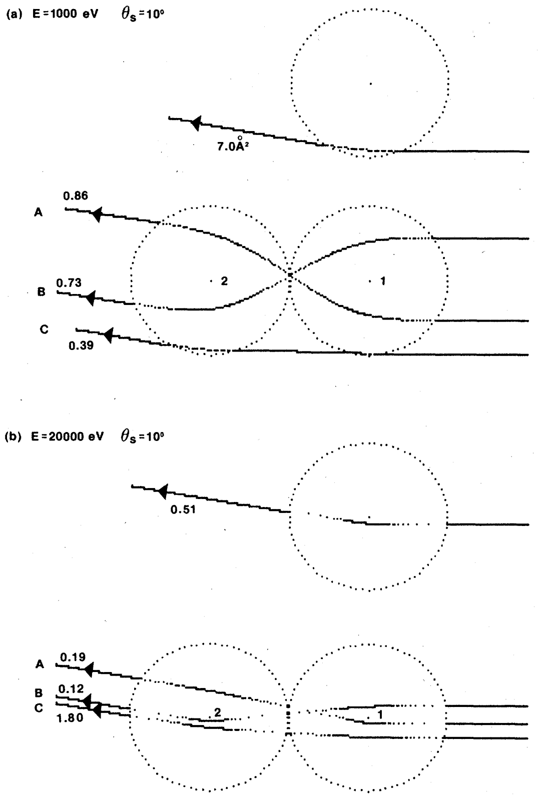

FIG. 4. Scattering by 10° of a parallel electron beam by one and two atoms: (a) electron energy = 1000 eV and (b) electron energy = 20 000 eV. The number on each ray is the classical differential cross section $d\sigma/d\Omega$.

III. LARGE-ANGLE SCATTERING SPECTROSCOPIES

We now turn to spectroscopies that collect electrons at large scattering angles: e.g., angle-resolved EDPD[7–10,29] and angular-dependent photoelectron spectroscopy (ADPD).[1] Recently, a number of works have used single-scattering theory to evaluate EDPD intensities at medium energies (100—600 eV).[14,30,31] At such energies, scattering amplitudes for angles larger than 25°—35° are small[32] and need to be kept only to first order (i.e., single scattering). Also, the forward-scattering cone gets smaller as electron energy increases. However, while multiple large-angle scatterings are small, a major error in single-scattering theory is that it uses the wrong wave front incident on atoms two or more neighbors away from the emission site. For example, referring to Fig. 1, the electron distribution after passing through one layer of atoms is the 2-ML curve, and not that of an unscattered wave.

We illustrate this situation in Fig. 5, where electrons emitted from a point source are scattered classically by a row of three atoms. The scattered electrons are collected at an angle of 150°. We calculate the differential count rate $d\tau/d\Omega$ which is defined as (see also the definition of τ above) the number of electrons scattered per second into $d\Omega$ divided by the number of electrons emitted by the source into $d\Omega$ per second, separately for atoms 1, 2, and 3 at 1000 eV (Fig. 5). The numbers indicate that at 1000 eV most electrons are scattered by atom 2. This is due to focusing of electrons onto atom 2 by atom 1. Single-scattering theory, on the other hand, would require each atom to have the same scattering factor as that of atom 1.

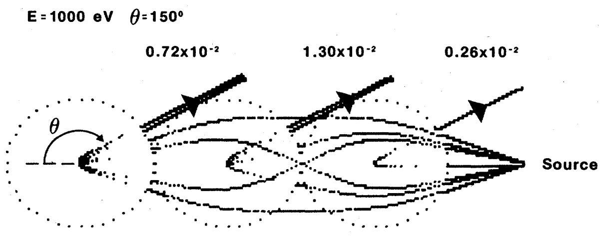

FIG. 5. Large-angle scattering at $\theta=150°$ of electrons emitted from a point source by three atoms: electron energy = 1000 eV. The number on each ray is the classical differential count rate $d\tau/d\Omega$.

With multiple scattering, it is shown that the relative scatterings from the various atoms are very different and that these are complex functions of energy and scattering angle.

Thus, for spectroscopies that count electrons at large scattering angles, single-scattering theory works if the crystal structure is very open and atoms beyond the nearest neighbors are not in the "cone of focusing" of the nearer atoms. The size of the focusing cone depends on the electron energy. To obtain accurate quantum-mechanical results for cases where many atoms are "shadowed," one could use the first-order quasidynamical method,[26,27] which includes multiple scatterings in the forward direction but keeps backscatterings only to first order, or one could use the multiple-scattering chain method of Masud and Pendry.[28]

IV. CONCLUSION

In summary, we have demonstrated the importance of multiple scattering in forward-direction and large-angle scattering spectroscopies. The forward-direction-enhanced peak in angle-resolved XPS or AES indicates that the scattered wave has an amplitude that is comparable to that of the unscattered wave. This causes the breakdown of the basic assumption of single-scattering theory: that the scattered wave's amplitude is small compared to that of the unscattered wave. Thus, one should use single-scattering theory only with caution (if at all), and depending on the scattering geometry and crystal structure, be wary of bond lengths and bond angles determined by intensity analysis from single-scattering theory. Even at medium or high energies, quantum-mechanical multiple-scattering methods must be used to give quantitatively reliable results.

Finally, our classical cross sections are not meant to be directly comparable with measured intensities. The cutoff Coulomb potential has a simple form and does not accurately represent surface potentials of solids. The classical cross section neglects interferences between rays. However, the classical analog is useful in demonstrating in a simple and pictorial way the qualitative differences between single- and multiple-scattering approaches. To make contact with measured intensities, quantum-mechanical multiple-forward-scattering methods must be used.

ACKNOWLEDGEMENTS

This work was supported in part by National Science Foundation Grant No. DMR-84-05049 and Petroleum Research Fund Grant No. 1154-AC5,6. The authors also wish to acknowledge useful discussions and correspondence with C. S. Fadley, M. A. Van Hove, and W. F. Egelhoff.

---

[1] See, for example, S. Y. Tong, Phys. Today, **37**(8), 50 (1984), and references therein.

[2] K. Siegbahn, U. Gelius, H. Siegbahn, and E. Olson, Phys. Lett. **32A**, 221 (1970).

[3] C. S. Fadley and S. A. L. Bergström, Phys. Lett. **35A**, 375 (1971).

[4] W. F. Egelhoff, Jr., J. Vac. Sci. Technol. A **2**, 350 (1984).

[5] W. F. Egelhoff, Jr., Phys. Rev. B **30**, 1052 (1982).

[6] W. F. Egelhoff, Jr., in *The Structure of Surfaces,* edited by S. Y. Tong and M. A. Van Hove (Springer, Berlin, 1985).

[7] S. D. Kevan, D. H. Rosenblatt, D. Denley, B. C. Lu, and D. A. Shirley, Phys. Rev. Lett. **41**, 1565 (1978).

[8] C. H. Li and S. Y. Tong, Phys. Rev. Lett. **42**, 901 (1979).

[9] S. Y. Tong and C. H. Li, J. Vac. Sci. Technol. **16**, 652 (1979).

[10] S. Y. Tong and C. H. Li, in *Chemistry and Physics of Solid Surfaces,* edited by R. Vanselow and W. England (Chemical Rubber Co., Cleveland, 1982), Vol. 3.

[11] C. S. Fadley, in *Progress in Surface Science,* edited by S. G. Davison (Pergamon, New York, 1984), and references therein.

[12] S. Kono, S. M. Goldberg, W. F. T. Hall, and C. S. Fadley, Phys. Rev. Lett. **41**, 1831 (1978).

[13] S. Kono, S. M. Goldberg, W. F. T. Hall, and C. S. Fadley, Phys. Rev. B **22**, 6085 (1980).

[14] E. L. Bullock, C. S. Fadley, and P. J. Orders, Phys. Rev. B **28**, 4867 (1983), and references therein.

[15] H. C. Poon and S. Y. Tong, Phys. Rev. B **30**, 6211 (1984).

[16] E. L. Bullock and C. S. Fadley, Phys. Rev. B **31**, 1212 (1985).

[17] R. A. Armstrong and W. F. Egelhoff, Surf. Sci. (to be published).

[18] S. Y. Tong, C. H. Li, and A. R. Lubinsky, Phys. Rev. Lett. **39**, 498 (1977).

[19] S. Y. Tong and C. H. Li, in *Critical Reviews in Solid States and Materials Sciences,* edited by D. E. Schuele and R. W. Hoffman (Chemical Rubber Co., Cleveland, 1981), Vol. 10, p. 209.

[20] C. H. Li, A. R. Lubinsky, and S. Y. Tong, Phys. Rev. B **17**, 3128 (1978).

[21] S. Y. Tong, W. M. Kang, D. H. Rosenblatt, J. G. Tobin, and D. A. Shirley, Phys. Rev. B **27**, 4632 (1983).

[22] Because of an inner potential of 12.8 eV, the maximum intensity actually occurs at 46.1° for 317 eV. At 917 eV, the maximum intensity occurs at 45.4°.

[23] J. E. Müller and W. L. Schaich, Phys. Rev. B **27**, 6489 (1983).

[24] W. M. MacDonald, Am. J. Phys. **41**, 1337 (1973).

[25] $d\tau/d\Omega \rightarrow \infty$ as $\Delta\theta \rightarrow 0$ in the classical model. However, τ in the forward direction is finite for a detector with finite size.

[26] S. Y. Tong, M. A. Van Hove, and B. J. Mrstik, in *Proceedings of the 7th International Vacuum Congress and 3rd International Conference on Solid Surfaces,* edited by R. Dobrozemsky *et al.* (Berger, Vienna, 1977), Vol. 3, p. 2407.

[27] C. H. Li and S. Y. Tong, Phys. Rev. Lett. **43**, 526 (1979).

[28] N. Masud and J. B. Pendry, J. Phys. C **9**, 1833 (1976).

[29] J. J. Barton, C. C. Bahr, Z. Hussain, S. W. Robey, J. G. Tobin, L. E. Klebanoff, and D. A. Shirley, Phys. Rev. Lett. **51**, 272 (1983).

[30] P. J. Orders and C. S. Fadley, Phys. Rev. B **27**, 781 (1983).

[31] M. Sagurton, E. L. Bullock, and C. S. Fadley, Phys. Rev. B **30**, 7332 (1984).

[32] S. Y. Tong, in *Progress in Surface Science,* edited by S. G. Davison (Pergamon, New York, 1975), Vol. 7, p. 1.